Synthesis, transport activity, membrane localization, and dynamics of oligoester ion channels containing diphenylacetylene units†

Joanne M. Moszynski and Thomas M. Fyles*

Received 1st June 2010, Accepted 10th August 2010
DOI: 10.1039/c0ob00194e

Four new linear oligoesters containing a diphenylacetylene unit were prepared by fragment coupling sequences and the ion channel forming ability of the compounds was investigated. Activity in vesicles was very strongly controlled by overall length; the longest compound was effectively inactive. Planar bilayer studies established that all compounds are able to form channels, but that regular step changes in conductance depend on the location of the diphenylacetylene unit within the oligoester and on the electrolyte. The intrinsic fluorescence of the diphenylacetylene unit was used to probe aggregation and membrane localization. Both monomer (320 nm) and excimer (380 nm) emissions are quenched by copper ions; quenching of the excimer emission from an aqueous aggregate is very efficient. Time-dependent changes in the intensities of monomer and excimer emission show slow transfer of diphenylacetylene units from an aqueous aggregate to a membrane-bound monomer with subsequent growth of emission from a membrane-bound excimer. The latter species is not quenched by aqueous copper ions. The implications of these species and processes for the mechanism of ion channel formation by simple oligoesters are discussed.

Introduction

Studies of the design and synthesis of synthetic ion channels over the past two decades have uncovered numerous examples of relatively simple compounds that can insert into a bilayer membrane and open ion conducting states (reviews;[1–3] recent examples[4–10]). Larger, rigid, or conformationally defined synthetic channel-forming compounds usually suggest a linkage between structures and possible mechanisms[11,12] and are amenable to structure–function study as a route to determining mechanistic details.[4,6,13,14] Simpler or more flexible compounds typically offer few structural clues to constrain mechanistic speculations.[15–19] Simpler compounds also offer fewer opportunities for innocent structural modifications to insert probes into the active compounds. As a consequence mechanistic hypotheses—as plausible as they might be—remain largely untested by direct experiment.

Such is certainly the case for the oligoester channel forming compounds reported recently.[20–22] A solid-phase synthesis gave easy access to a suite of these compounds and a structure–activity survey directed attention to a mechanism in which the transport activity was controlled by aqueous-phase aggregation of the compound prior to membrane insertion (Fig. 1).[20] The aggregation of the compounds was probed indirectly and generally supported the view that the most active compounds aggregated to the least extent thereby increasing the available monomer for partition to the membrane.[20] Subsequent channel opening was presumed to occur *via* a dimeric or oligomeric *trans*-membrane species which stabilized an aqueous pore through which ions could travel, in line with earlier proposals.[23]

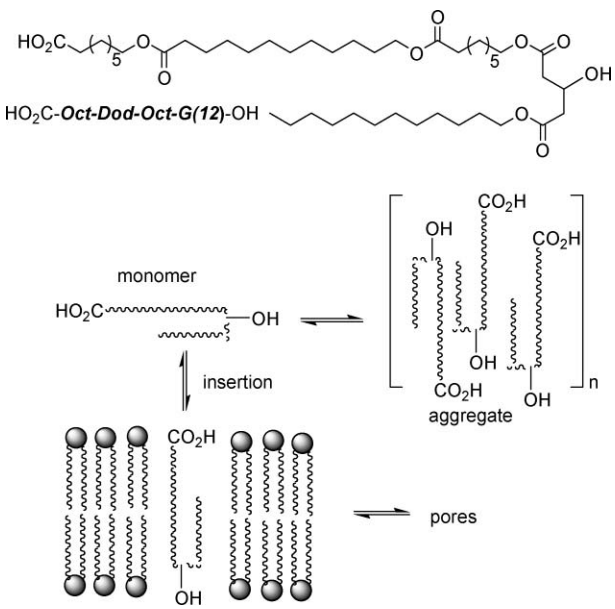

Fig. 1 Working hypothesis for the formation of ion channels.

The working hypothesis has much in common with proposals for the channel-forming activity of conventional detergents,[24] and may be relevant to the modes of action of a number of other very simple channel-forming compounds.[10,25] The membrane-spanning oligoesters are also inherently dipolar, a necessary condition for voltage-response functions of synthetic channels.[26–28] Consequently, a current focus is to directly test this mechanistic framework in the expectation that higher-order membrane functions, such as excitable membrane phenomena, will become practicable based on inherently simple syntheses.

Department of Chemistry, University of Victoria, PO Box 3065, Victoria, BC, Canada. E-mail: tmf@uvic.ca; Fax: +1 250 721 7147; Tel: +1 250 721 7192

† Electronic supplementary information (ESI) available: Details of synthesis and purifications, ^{1}H and ^{13}C NMR, HPLC traces and MS spectra for all new compounds; rate data determined from HPTS assay for final oligomers; fluorescence and fluorescence quenching experimental data as referred to in the text. See DOI: 10.1039/c0ob00194e

In an effort to find more active compounds, our focus was on the assumed rate-limiting process of monomer partition from aqueous solution to the bilayer. The rate of this step can be controlled through the monomer concentration in equilibrium with an aqueous aggregate as was inferred in the previous report.[20] It should also be possible to directly influence the rate of partition *via* incorporation of rigid elements within the oligoester; rigid units have previously been implicated as elements of ion channel designs,[2,3] and rigidification can contribute to control of channel stability.[13] In the oligoester system, a rigidifying element would be expected to influence the activity in two ways: acceleration of the partition step in the forward direction, and *via* destabilization of the aggregate thereby increasing the equilibrium monomer concentration.[29] Introduction of a rigid unit also offers the potential to incorporate an intrinsic environmental probe into the target.[30]

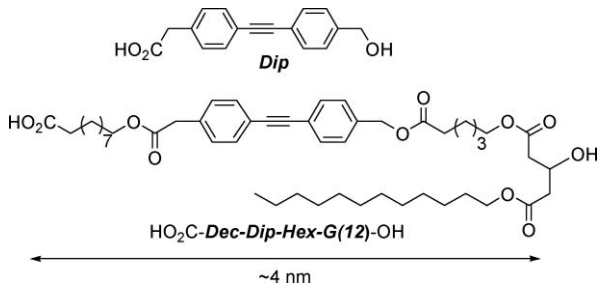

Accordingly we focused on a diphenylacetylene containing α,ω-hydroxy acid (***Dip***) subunit that we envisaged as being introduced into the suite of known oligoester channels using the previously reported solid-phase synthesis protocols and subunits. In addition, the diphenylacetylene unit would provide a useful chromophore to assist in purification and characterization of the final products, and more importantly to provide a sensitive spectroscopic probe of membrane localization and dynamics through fluorescence. The origin of the luminescence of the parent diphenylacetylene is complex[31,32] but this has not inhibited its use as a spectroscopic probe.[33] Excitation of dilute solutions of diphenylacetylene at 280 nm results in a monomer emission maximum at 320 nm; in more concentrated solutions a broad excimer emission about 380 nm can be observed.[32,33] Both the monomer and excimer emissions can be quenched, although the suite of known quenchers is limited.[32]

The ***Dip*** subunit has a carbonyl to hydroxyl length of 1.43 nm, midway between the estimated lengths of 1.14 nm and 1.65 nm in the extended conformations of the 8-hydroxyoctanoic acid and 12-hydroxydodecanoic acid subunits previously incorporated into oligoester channels.‡ The previous work did not uncover a marked dependence of activity on overall length, and flexible structures have the possibility of overall shortening due to *gauche* conformations within the chains. The homolog pictured above has an approximate length of 4 nm, within the range required to span a bilayer membrane.

‡ The trivial naming of the compounds follows from the linear structures with the carboxy and hydroxy termini explicitly specified; named subunits are assumed to be linked as esters. The ***G(n)*** unit indicates a diester of 3-hydroxy glutaric acid with an n-carbon alkyl ester. The α,ω-hydroxyacids of 6, 8, 10, and 12 carbons are indicated as ***Hex***, ***Oct***, ***Dec***, and ***Dod*** respectively. In this paper only the final structures are named this way.

The goals of this paper are to report the synthetic studies that produce the required oligoesters containing the ***Dip*** subunit, to establish the membrane activity of the new compounds relative to more flexible relatives prepared previously, and to exploit the fluorescence properties of the compounds to probe the mechanistic framework in which these compounds act.

Synthesis

The diphenylacetylene derivative required for the projected targets (**3**) was readily prepared by Sonogashira coupling[34] of the known iodo-acid **1** and the protected terminal acetylene **2** as shown in Scheme 1. A modest excess of **1** with respect to **2** over a $Pd(PPh_3)_4/CuI/NEt_3$ catalyst mixture in DMF, followed by extractive workup and purification by silica gel chromatography gave the product in an average 85% yield (multiple preparations) as clear, colourless crystals. However, all attempts to use **3** in a solid-phase synthesis based upon previously established protocols for coupling and cleavage gave complex mixtures with several components containing chromophores. It was possible to establish that **3** coupled very slowly with alcohols on the support resin, and

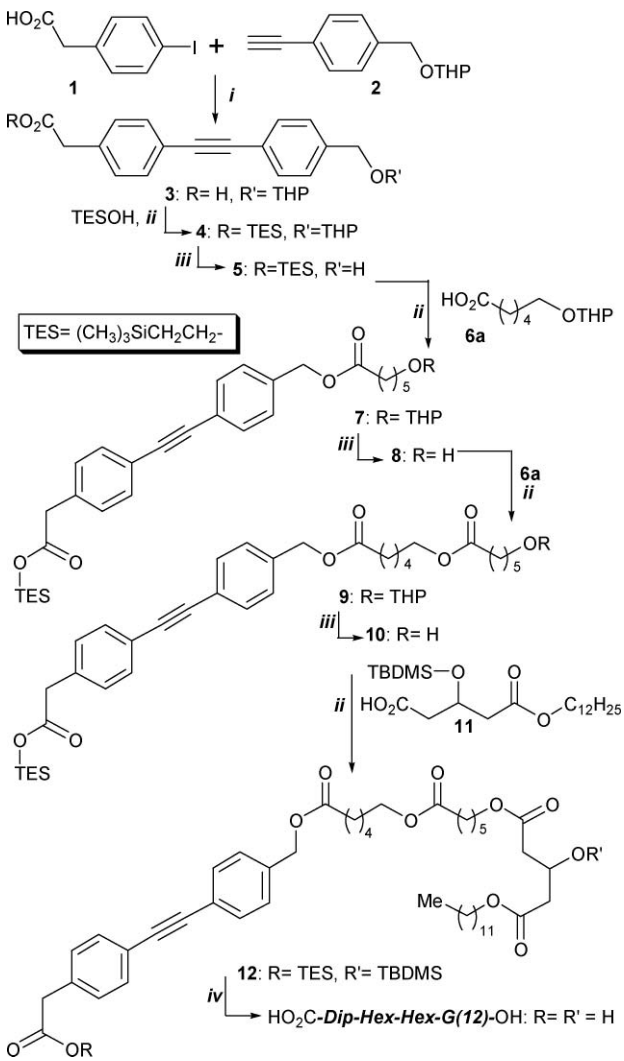

Scheme 1 Synthesis of HO_2C-***Dip-Hex-Hex-G(12)***–OH.§

it also appears likely that a significant portion of the acetylene does not survive the acidic cleavage conditions.

We therefore turned to a solution synthesis of the same overall design in which the final oligoester would be built from the carboxyl terminus towards the hydroxy terminus. The solution synthesis follows a similar set of standard reaction protocols for ester coupling and deprotection steps; the only exception is that workup is compound specific as opposed to the filtration/washing procedure of the solid-phase method. The solution synthesis requires a carboxylic acid protecting group with properties orthogonal to tetrahydropyranyl (THP). The trimethylsilyloxyethyl (TES) group[35] appeared to fulfil the requirements; it is stable to mild acid conditions but is cleaved by fluoride. An alternative for carboxylic acid protection is the allylic ester derived from isoprene (PRE) that is readily cleaved with trimethylsilyl triflate to give volatile by-products on workup.[35] In both cases the required starting materials were prepared by coupling a THP-protected hydroxy acid *e.g.* **6a** with the required alcohol under standard esterification conditions followed by standard THP deprotection. A key to standard reaction conditions and protected species is given in a footnote.§

Scheme 1 shows the synthesis of the tetramer HO_2C-***Dip-Hex-Hex-G(12)***–OH. This synthesis mimics the solid-phase method through a sequential application of an acidic deprotection to remove the THP followed by a standard coupling with a THP protected hydroxy acid. Two deprotection-coupling cycles with the six-carbon hydroxyacid **6a** gave successively compounds **7**/**8** and **9**/**10**. It was convenient to purify the doubly protected species **7** and **9** as deprotection is essentially quantitative and the products **8** and **10** could be used without purification.

The two-step sequences **6a** to **8** and **8** to **10** occurred in yields of 76% and 72% respectively. The final coupling was accomplished with the TBDMS protected hydroxyglutaric half ester **11** to give the fully protected tetramer **12**. A final deprotection with fluoride cleaved both the TES and TBDMS groups to produce the required hydroxy acid HO_2C-***Dip-Hex-Hex-G(12)***–OH in 17% yield from **3**.

This is a rigorous mimic of the unachievable solid-phase synthesis. The eight chemical steps produce seven intermediates, which unlike a solid phase synthesis are isolated and identified. This additional effort eliminates any incomplete coupling products and the final product is readily purified by preparative HPLC with concurrent absorbance and fluorescence detection to produce the tetramer in substantially higher purity than would have been possible with the solid-phase methodology. A comparable sequence by solid-phase would take less than a week to complete including final gel permeation chromatography; the manipulations required for Scheme 1 take four weeks and involve six chromatographic separations.

Although a preformed diphenylacetylene such as **3** is required for a solid-phase synthesis, it is not a requirement for a solution synthesis. Moreover, the Sonogashira coupling offers an efficiency advantage compared to the rather sluggish esterification reactions involving **3**. A synthesis that explores improvements to the synthesis of Scheme 1 is given in Scheme 2 for the isomeric HO_2C-***Hex-Hex-Dip-G(12)***–OH.

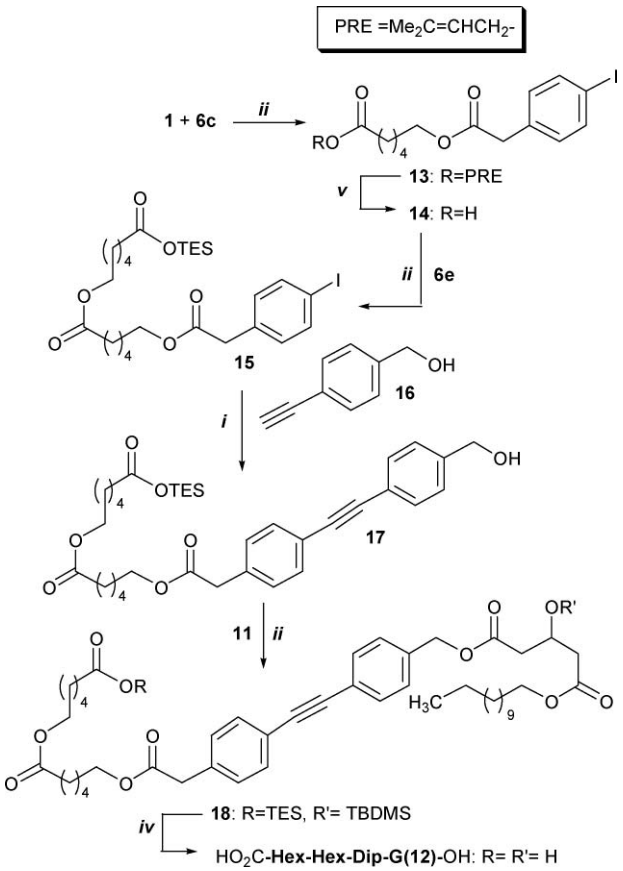

Scheme 2 Synthesis of HO_2C-***Hex-Hex-Dip-G(12)***–OH.§

Any synthesis to place the ***Dip*** subunit at an internal oligoester position requires a free hydroxyl group at some point. Although this can be accomplished with the TES/THP combination, the fluoride deprotection step is best followed by a chromatographic purification due to impurities in the reagent. A cleaner deprotection process could potentially eliminate this chromatographic step.

Starting from the THP protected hydroxyhexanoic acid **6a**, the PRE protecting group was installed in good yield using the standard esterification protocol. A standard acidic cleavage of the THP group in **6b** gave the required alcohol **6c** which was extended with the iodoacid **1** to give a PRE protected compound **13** (Scheme 2). Deprotection with TMSOTf was undertaken to allow the extension of the ester chain from the carboxylic acid terminus. As expected, the deprotection product **14** was suitable for the next step without additional purification. The subsequent coupling with **6e** (from **6a** by a TES protect/THP deprotect sequence) gave the Sonogashira precursor **15**.

The coupling with the acetylenic alcohol gave the hydroxy-terminated trimer **17** that was extended to the fully protected tetramer **18**. As previously, both protecting groups were removed in a single fluoride treatment to give the target HO_2C-***Hex-Hex-Dip-G(12)***–OH in an overall yield of 21% over 6 steps from **1**. This synthesis is one step shorter than the linear sequence of

§ Conditions: (***i***) Pd(0), CuI, NEt_3, DMF or THF, rt → 50 °C; (***ii***) DIC, DiPEA, HOBt, THF, rt → 50 °C; (***iii***) TsOH, CH_2Cl_2–CH_3OH, rt; (***iv***) TBAF, THF, rt; (***v***) TMSOTf, CH_2Cl_2, rt. Compound **6**: RO_2C-$(CH_2)_5$-OR′. **6a**: R = H, R′ = THP. **6b**: R = PRE, R′ = THP, **6c**: R = PRE, R′ = H. **6d**: R = TES, R′ = THP, **6e**: R = TES, R′ = H. Compound **24**: RO_2C-$(CH_2)_9$-OR′: **24a**: R = H, R′ = THP, **24b**: R = PRE, R′ = THP, **24c**: R = PRE, R′ = H

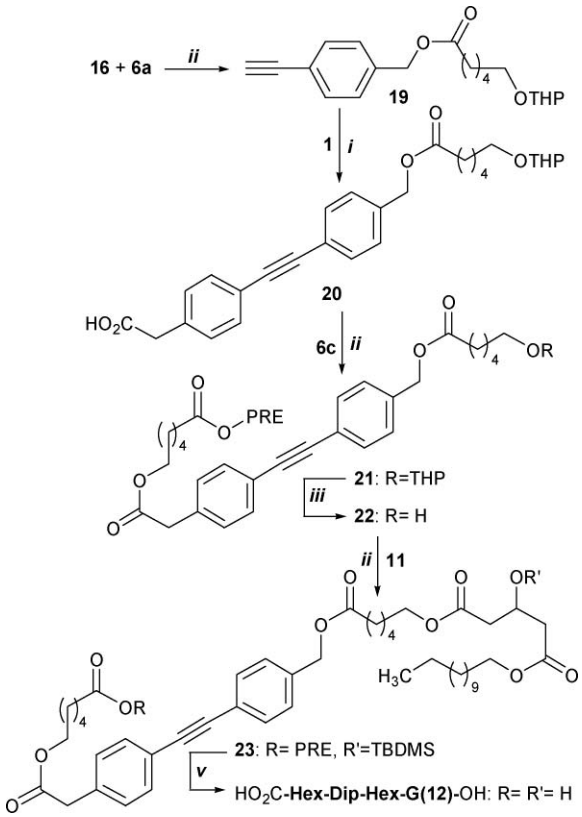

Scheme 3 Synthesis of HO_2C-***Hex-Dip-Hex-G(12)***–OH.§

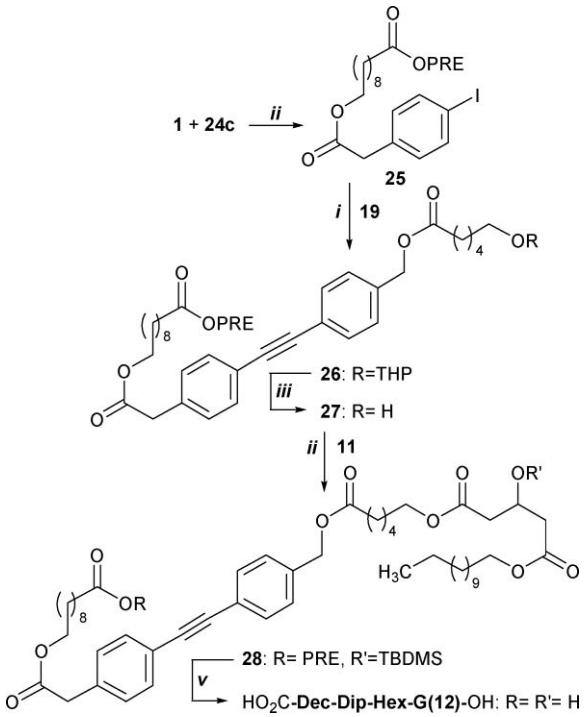

Scheme 4 Synthesis of HO_2C-***Dec-Dip-Hex-G(12)***–OH.§

Scheme 1 by virtue of the Sonogashira coupling on an unprotected alcohol. On a practical level it also reveals the advantage of the PRE protecting group compared to TES. Nonetheless, this route is also a linear sequence that proceeds from the carboxylic acid towards the hydroxy terminus.

Scheme 3 shows a third strategy for the preparation of the final sequence isomer HO_2C-***Hex-Dip-Hex-G(12)***–OH containing the ***Dip*** group in the central position. This route produces a trimer strand for final coupling to the ***G(12)*** unit *via* chain growth from the hydroxyl to the carboxyl terminus. In this sequence the hydroxy protected acid **6a** is converted to the terminal alkyne **19** which then is coupled with the iodoacid **1** to give the free acid **20**. The trimer is completed through ester coupling with the PRE protected subunit **6c**.

The final stages of the synthesis require THP cleavage to open an alcohol for coupling with the protected ***G(12)*** subunit to give **23**. On treatment with TMSOTf, the fully protected product **23** lost both the PRE and TBDMS protecting groups to give HO_2C-***Hex-Dip-Hex-G(12)***–OH in good yield and purity. The simultaneous cleavage of PRE and TBDMS is general and provides a clean and convenient means to complete the synthesis, leading to an overall yield of 14% over 6 steps from **16**.

The routes explored in Schemes 1–3 all involve coupling of low molecular weight acetylene precursors to ester chains of various sizes. A more convergent strategy would involve Sonogashira coupling uniting two similarly-sized ester components. This type of route is given in Scheme 4. The target is the longer homolog HO_2C-***Dec-Dip-Hex-G(12)***–OH with the diphenylacetylene at the centre of the trimer strand. The final stages of Schemes 3 and 4 are the same; a ***G(12)*** unit is coupled with a hydroxy terminated trimer **27** and the protected product **28** is deprotected in a single step.

The earlier stages of the synthesis were complicated by the apparent instability and poor reactivity of the THP-protected ten carbon fragment **24a**, a precursor of the required building block **24c**. However, once obtained, **24c** was seen to undergo efficient coupling with **1** to yield the aromatic iodide **25**. In the key event, the coupling with the terminal alkyne **19** produced the expected internal alkyne **26** in 85% yield. The remaining steps of the synthesis proceeded in good yields to give the target in 41% overall yield from **1**.

Although the manipulations in the solid-phase synthesis are undoubtedly fewer and easier, the solution syntheses reported here have significant advantages. These derive directly from the incorporated chromophore/fluorophore that greatly improves the detection of products of interest. All compounds are readily purified by HPLC to give single component samples. This eliminates the combination NMR/MS analysis used previously to estimate sample purity. The structure of the synthesis varies, as shown in the Schemes, but the repertoire of reactions is highly standardized and reliable. Like the solid-phase, these methods are sequence independent and applicable for the synthesis of any desired homolog.

Transport studies in vesicles

The activity of the compounds was assessed using the HPTS assay technique[1] with the local variants reported previously.[20] In this method, vesicles are prepared with the pH-sensitive dye HPTS entrapped. The initial mixture of vesicles and added transporter shows stable fluorescence. Transport is initiated by the injection of a pulse of base to create a transmembrane pH gradient that

collapses due to transport through the membrane mediated by added transporter. Alternate excitation at 403 and 460 nm excites the acid and conjugate base forms of the dye respectively which both emit at 510 nm. The modulated output signal can be converted to a normalized extent of transport using the procedure described previously.[20]

Fig. 2(A) shows the data for a transport experiment for varying concentrations of HO_2C-***Dip-Hex-Hex-G(12)***–OH. The most striking result is the substantially higher activity of this compound relative to all the compounds previously reported. In the previous work, mid-range activity was reported for a concentration of 32 μM; the activity of HO_2C-***Dip-Hex-Hex-G(12)***–OH is significant at a five-fold lower concentration. At low concentrations, the transport curves are very similar to those previously reported. There is an initial fast "jump" process following the pH pulse followed by a linear section. The fast process is the adjustment of the vesicles to ionic and osmotic stresses *via* random pore formation within the bilayer that results in some pH equilibration. The slower linear process is the solution-diffusion regime which is accelerated by added transporter.[36] However, at higher concentrations the curves are clearly never linear functions of time, but can be fit with high significance to an apparent first-order function (r-squared > 0.99). The transition from zero- to first-order behaviour is a very abrupt function of concentration.

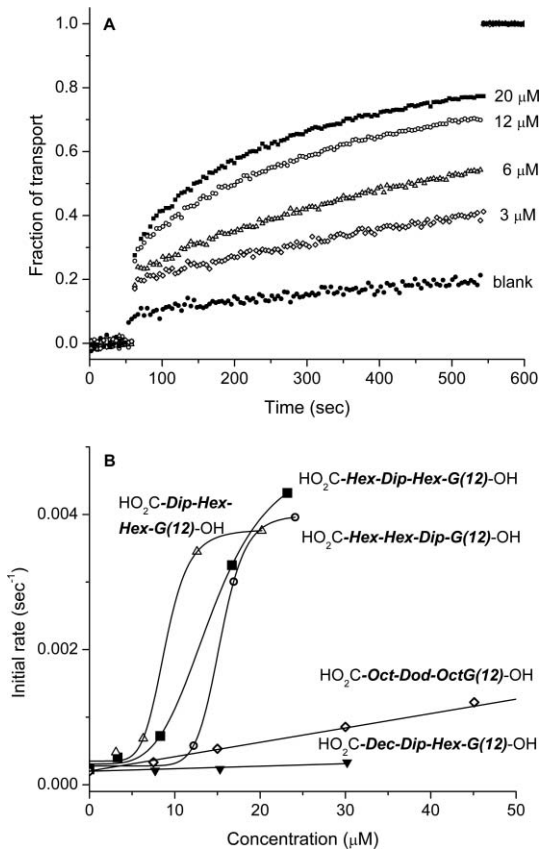

Fig. 2 Transport by ***Dip***-containing oligoesters in vesicles containing HPTS. A: Fraction of transport as a function of time for various concentrations of HO_2C-***Dip-Hex-Hex-G(12)***–OH; B: Initial rate following hydroxide gradient creation as a function of concentration for compounds considered.

Either zero- or first-order fitting results can be used to extrapolate an apparent initial rate at the time of the pH pulse (see the ESI†). This procedure allows comparison over a range of concentrations for the various compounds. The results are presented in Fig. 2(B) which emphasizes the point made above; that the positional isomers of HO_2C-***Dip-Hex-Hex-G(12)***–OH all show a sharp increase in initial rate at a concentration between 5 and 20 μM. In contrast, the previously reported compound HO_2C-***Oct-Dod-Oct-G(10)***–OH still behaves as originally reported. The transport rate constant derived at 32μM from these data is 8.4×10^{-4} s^{-1} in reasonable comparison to the value of $(6.3 \pm 2.1) \times 10^{-4}$ s^{-1} reported.[20]

Fig. 2(B) shows fits for the most active compounds to a logistic function of the type used previously to characterize aggregation behaviour.[20] The fitting equation is functionally equivalent to the Hill equation used to characterize the concentration dependence of ion channels.[1] The derived Hill coefficients range from 4 to 11, indicating significant aggregation within the membrane as a rate-limiting condition of transport activity. The apparent dissociation constants of the active species range from 9–15 μM.

Another striking result from Fig. 2(B) is the very low activity of HO_2C-***Dec-Dip-Hex-G(12)***–OH. In the previous study it would have been at the borderline of significant activity. This is a remarkable effect of length. Several reported systems reveal a variation in activity as function of transporter length and this has been exploited as a probe of membrane thickness.[37] The very large activity difference between homologs differing by four methylene groups is unprecedented.

Transport in planar bilayers

The transport activity of the compounds was also assessed in diphytanoylphosphatidylcholine (diPhyPC) planar bilayers by the voltage-clamp technique.[38–41] None of the compounds produced detectible activity by direct injection of compound in methanol or THF solution into the electrolyte solutions contacting the planar bilayer. Rather, the compound, typically at 0.3 mol% in lipid, was physically transferred to a formed bilayer. Alternatively, bilayers could be formed from lipid containing compound. All bilayers were monitored to ensure high capacitance/high resistance barriers were continuously present.

The array of observed conductance behaviours is given in Fig. 3; there is a range of behaviours represented, but each is reliably produced by the compound/electrolyte combination presented. Nearly ideally behaved single channels were observed for HO_2C-***Hex-Dip-Hex-G(12)***–OH with CsCl electrolyte (Fig. 3(A) and 3(B)). These channels are Ohmic with a conductance of 140 ± 3 pS, a lifetime of the order of 700 msec, and an open probability within the first 30 min of activity of 7%. The activity persists for hours with increasing open probability that eventually results in coalescence to a single persistent opening. Multiple levels are not observed until the persistent opening is established. The longer homolog HO_2C-***Dec-Dip-Hex-G(12)***–OH is markedly different but also very well-behaved as shown in Fig. 3(C). In this case the channels have a conductance of 26 ± 3 pS, a lifetime of 5.7 msec and an open probability of 56%. This flickering behaviour persists for periods of hours and eventually progresses to an essentially continuously open state and then to multiples of this opening.

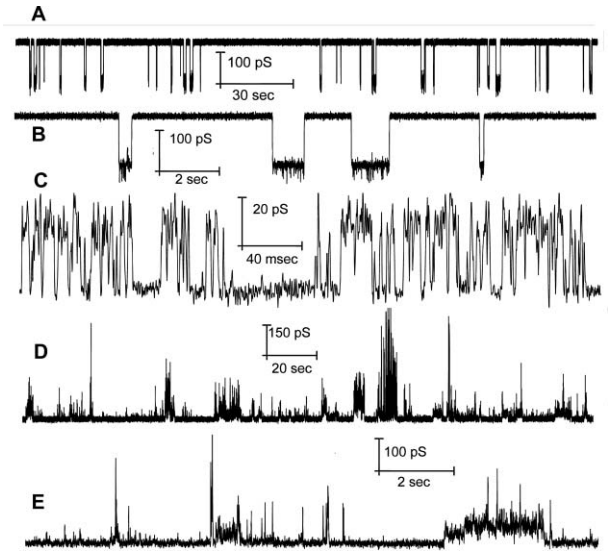

Fig. 3 Voltage-clamp traces of current as a function of time. A, B: HO_2C-***Hex-Dip-Hex-G(12)***–OH in diPhyPC/1M CsCl/–175 mV; C: HO_2C-***Dec-Dip-Hex-G(12)***–OH/1M CsCl/+175 mV; D, E: HO_2C-***Hex-Hex- Dip-G(12)***–OH/1M KCl/60 mV.

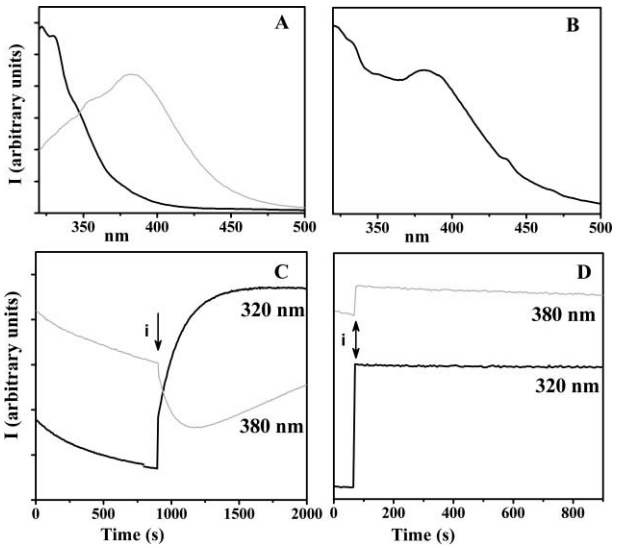

Fig. 4 Fluorescence characteristics of **Dip**-containing oligoesters. (A) Fluorescence spectra (λ_{ex} = 305 nm) of HO_2C-***Dip-Hex-Hex-G(12)***–OH in THF (black line) or aqueous solution (10 mM phosphate buffer, pH = 6.4, 100 mM NaCl, grey line). (B) Fluorescence spectrum of the same compound in aqueous solution following addition of lipid vesicles (after a 30 min equilibration period). (C) Time dependence of emission intensity at 320 and 380 nm for HO_2C-***Dip-Hex-Hex-G(12)***–OH; i marks the introduction of lipid vesicles. (D) Same experiment as in (C) for HO_2C-***Dec-Dip-Hex-G(12)***–OH.

The other classes of behaviours observed are shown in Fig. 3 sections D and E. These were obtained with HO_2C-***Hex-Hex-Dip-G(12)***–OH and KCl as electrolyte, but all compounds show this type of behaviour with KCl, and this isomer also shows this behaviour with CsCl electrolyte. The dominant characteristic of these records is a series of short "spikes" of highly variable conductance. The spikes typically occur directly from the baseline but their short duration, high conductance, and relatively high frequency can result in an envelope of high conductance. This is probably an artefact of the acquisition and hardware filtering speed; it is highly likely the spikes are individually very short duration (<msec) openings of highly varied conductance. In some cases these appear to be associated with, or occurring in addition to, a step-conductance state as illustrated in Fig. 3(E). In these cases, the apparent underlying step conductance state increases in duration and leads eventually to a continuously open condition with spikes of variable magnitude superimposed. The underlying level, if it is indeed a discrete state, can be detected in an all-points histogram as a main feature with a long tail to higher absolute conductance. The magnitude of the underlying level varies considerably in the range of 150–700 pS. There is no evidence of discrete values within this range. Given that the electrolyte influences the type of activity observed, a selectivity study is not possible in this system. Similarly, the incorporation method precludes investigation of voltage-gating.

The Hille equation[42] relates the observed conductance to an apparent radius of the ion channel.[39] Based on an assumed channel length of 3.4 nm, the openings of Fig. 3(A) have an apparent radius of 0.31 nm while the smaller conductance changes in Fig. 3(C) have an apparent radius of 0.11 nm. On the same assumptions, the spikes must have radii up to 1 nm. The underlying step-conductance features give radii in the range 0.34–0.45 nm for the four compounds in KCl electrolyte.

Fluorescence studies

Diphenylacetylene is inherently fluorescent;[32] in THF solution the expected monomer emission at 320 nm is readily observed for all four compounds (Fig. 4(A)). This band is absent in aqueous buffer, and the emission shifts to 380 nm, a region previously associated with excimer formation (Fig. 4(A)).[32] The excimer arises from an aggregate. The aggregate species can be detected from the solvent polarity dependent pyrene emission spectrum as used previously,[20,43] which indicates that a hydrophobic aggregate forms at a concentration below 20μM (see the ESI†). The overall excimer emission intensity falls slowly with time as the aggregate species initially formed by injection of a solution of compound in THF is not in a stable state in aqueous solution.

The addition of a vesicle solution to the aggregate formed by HO_2C-***Dip-Hex-Hex-G(12)***–OH in aqueous buffer provokes a time-dependent change in the emission spectra as illustrated in Fig. 4(B) and 4(C). At early times following vesicle addition, the excimer emission intensity decreases while the monomer emission intensity abruptly increases. Later, the excimer band regains intensity. These time dependent changes are plotted in Fig. 4(C) for the emission maxima at 320 and 380 nm. The static spectrum at 30 min (Fig. 4(B)) appears as a sum of the monomer and excimer spectra. The alternate sequence (injection of compound to a solution that already contains vesicles) results in spectra that are comparable to Fig. 4(B) and evolve as the right-hand portion of Fig. 4(C). Over long times, the final state is independent of the sequence of mixing but progress to the final state is slow (minutes to hours).

We interpret the time-dependent sequence of Fig. 4(C) as follows. Before the addition of vesicles, the aggregate in water is

unstable and slowly evolves in structure which alters the emission spectra. Upon vesicle addition, available aqueous monomer is rapidly partitioned to the vesicle where it can emit; a portion of the immediate intensity change is also due to a change in the scattering of the solution. The monomer emission observed must arise predominantly from the compound in vesicles, and increases over time as compound migrates from the aqueous phase. Partition of monomer depletes the amount of aqueous aggregate thereby increasing the monomer emission intensity at the expense of the excimer emission intensity. The slow decline over the 200 s following vesicle addition, followed by reversal, indicates that the rate is controlled by the disassembly of the aqueous aggregate. Eventually, the monomer concentration in the vesicle bilayer grows to a concentration where excimer within the bilayer can form. Thereafter the monomer concentration in the bilayer reaches a steady state while the excimer emission intensity increases as further dissolution of aqueous aggregate proceeds. In the limit, the excimer and monomer emissions will become constant as the compound is fully dispersed between its various states in the microheterogeneous mixture.

In contrast, the corresponding spectra for the longest compound (HO_2C-***Dec-Dip-Hex-G(12)***–OH; Fig. 4(D)) show a sharp change on vesicle addition, but thereafter the migration dynamics are either very much slower (or faster) as the system does not appear to evolve at all; quenching studies (see below) establish that HO_2C-***Dec-Dip-Hex-G(12)***–OH undergoes very slow transfer from aggregate to vesicle. The positional isomers of HO_2C-***Dip-Hex-Hex-G(12)***–OH lie between the two extremes of Fig. 4(C) and 4(D); they appear to transfer somewhat more slowly than HO_2C-***Dec-Dip-Hex-G(12)***–OH, but clearly do transfer from an aggregate in water to a vesicle environment (see the ESI†).

The rates of these redistribution processes are slow; do they have any relevance to the transport processes detected using an HPTS assay? The fluorescence of the ***Dip***-containing compound can be monitored concurrently with the HPTS assay. The results (see the ESI†) confirm that the transport process for an active compound such as HO_2C-***Dip-Hex-Hex-G(12)***–OH and the redistribution process occur concurrently. Redistribution is slower than the collapse of the pH gradient reported by the HPTS assay; in a zero order case the derived rate would not be significantly influenced while the apparent first-order rate will incorporate the two but be dominated by the transport.

An examination of the fluorescence quenching behaviours was expected to yield information on the localization of the fluorophore. If the ***Dip*** was located deep in a hydrophobic region it should be relatively inefficiently quenched by a hydrophilic quencher in the aqueous phase. After some initial trials, the quenching by aqueous copper(II) was chosen for systematic examination. In homogeneous methanol solution quenching of the monomer (320 nm) emission occurs in the range of 0.1–1 mM added $CuSO_4$ to yield Stern–Volmer constants of about 1×10^3 M^{-1} (see the ESI†). This order of magnitude is consistent with a simple diffusion controlled quenching of an excited state with a lifetime of the order of nanoseconds as previously determined.[32] The differences between the compounds are negligible in comparison to the dramatically more efficient quenching of the excimer emission of aqueous aggregates by $CuSO_4$ in the concentration range of 0.1–1 μM (see the ESI†). The system involving aggregates has complex dynamics and a substantial static quenching contribution. The excimer/aggregate near neutral pH would be a polyanionic species, so an electrostatic association of the divalent copper ion to this aggregate is very likely. This would produce a very efficient quenching at low concentrations of copper. A similar mechanism has been reported for the efficient quenching of conjugated anionic polyelectrolyte aggregates based on poly(phenylene ethynylene) by micromolar cationic quencher concentrations.[44] The quenching by copper is pH dependent with higher copper concentrations required as the pH and buffer concentrations increase (see the ESI†).

Key experiments are illustrated in Fig. 5; compound (HO_2C-***Dip-Hex-Hex-G(12)***–OH in Fig. 5(A); HO_2C-***Dec-Dip-Hex-G(12)***–OH in Fig. 5(B)) was added to aqueous solution and the aggregation process was allowed to occur over a 5 min period, followed by injection of vesicles and a further period of redistribution. At this point, aqueous $CuSO_4$ was added to a final concentration of 1 μM. In the case of HO_2C-***Dip-Hex-Hex-G(12)***–OH there is a small dilution perturbation to the emission spectrum, but excimer fluorescence at 380 nm is virtually unchanged. In contrast, the excimer emission from the system containing HO_2C-***Dec-Dip-Hex-G(12)***–OH is substantially quenched by the aqueous copper. In both cases, the observed monomer emission is only changed by a dilution factor as the copper concentration is well below the level at which monomer quenching could be expected even if the monomer were completely accessible to the quencher.

Fig. 5(C) and 5(D) illustrate the effect of added copper ion on the full emission spectrum; while HO_2C-***Dip-Hex-Hex-G(12)***–OH is markedly quenched in water (4C(a)) and unquenched in vesicles (4C(b)), HO_2C-***Dec-Dip-Hex-G(12)***–OH undergoes almost identical extent of quenching whether in water alone (4D(a)) or in the presence of vesicles (4D(b)). The quenching experiments can also be conducted under conditions where the compounds and vesicles are mixed in the inverse order (see the

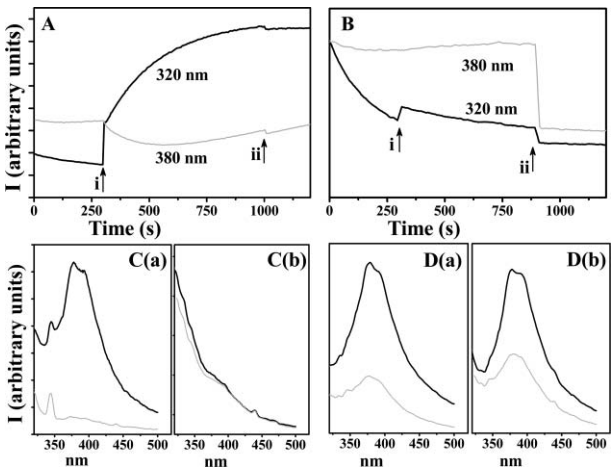

Fig. 5 *Upper panel*: time-based emission at 320 and 380 nm for (A) HO_2C-***Dip-Hex-Hex-G(12)***–OH and (B) HO_2C-***Dec-Dip-Hex-G(12)***–OH, (λ_{ex} = 305 nm). The compounds are initially in aqueous solution (0.1 M NaCl, unbuffered), to which lipid vesicles (time i) and 1 μM $CuSO_4$ (time ii) are added. *Lower panel*: fluorescence spectra of (C) HO_2C-***Dip-Hex-Hex-G(12)***–OH and (D) HO_2C-***Dec-Dip-Hex-G(12)***–OH, (λ_{ex} = 305 nm) in aqueous solution (a), or with the addition of lipid vesicles (b), in the absence (black lines) or presence (grey lines) of 1 μM $CuSO_4$.

ESI†). The sequence homologs of HO_2C-***Dip-Hex-Hex-G(12)***–OH all behave similarly in that excimer emission after some period in contact with vesicles cannot be significantly quenched by low levels of copper. The compound HO_2C-***Dec-Dip-Hex-G(12)***–OH can be incorporated into vesicles during preparation. Under these conditions there is strong monomer fluorescence at 320 nm (see the ESI†). The intensity of the excimer emission from these vesicles is too low for a copper ion quenching study; the monomer emission is not quenched up to 1 mM added $CuSO_4$.

A simple interpretation of these results is that the lack of quenching by copper ion indicates a membrane location of the compound such that the excimer is no longer accessible to aqueous quencher, due to incorporation in a hydrophobic region of the bilayer. In the case where quenching in the presence of vesicles is observed, the excimer would arise from aqueous-phase aggregate that has not redistributed to the vesicle bilayer. This interpretation has clear mechanistic implications, but must be handled with caution as the role of static quenching has not yet been fully elucidated.

Discussion and conclusions

Mechanistic proposals for the formation of ion channels from flexible acyclic compounds similar to the ones discussed here have centred primarily on the structure of the active species.[24,25,45,46] Although this is certainly an interesting issue, "mechanism" in this context also involves a number of other aspects: which species are present in the system, how do they interconvert, what are the relative energies and rates of interconversion?[1–3] The framework sketched in Fig. 1 is focused on this latter set of questions and the collection of data presented in this report probes these questions directly. Bilayer-bound states are required by the transport results that show that all four compounds are capable of provoking channel behaviour when premixed in lipid as detected by the voltage clamp technique. The proposed[20] aqueous phase aggregate is directly observed in solutions without vesicles as well as in contact with vesicles (pyrene assay, excimer fluorescence). A membrane associated monomer can be formed by incorporation during vesicle preparation for HO_2C-***Dec-Dip-Hex-G(12)***–OH, or by transfer from aqueous solution in the case of the other three compounds. The aqueous aggregates in the absence of vesicles for all four compounds show relatively weak monomer fluorescence; therefore the monomer emissions observed in the presence of vesicles must be due to a membrane-associated monomer. Finally, the time-dependent and quenching experiments reported suggest the rates at which the various equilibria can operate. Thus the species and processes identified in Fig. 1 now have some experimental basis.

The aqueous phase aggregate is in competition with, and controls, the transport process. This is clear in the case of HO_2C-***Dec-Dip-Hex-G(12)***–OH in vesicles which stalls as the aqueous aggregate and does not progress to membrane incorporation. This results in this compound appearing to be inactive in the vesicle transport assay, even though it is certainly capable of forming channels once it is in a lipid bilayer. The other compounds are more active in vesicles, but even in these cases the transfer of material from an aqueous aggregate to a vesicle bilayer is a relatively slow process as shown by the time dependence of the fluorescence changes that accompany this process. We continue to assume that the intermediate is an aqueous monomer as given in Fig. 1, but there is no direct spectroscopic evidence for this species.

Turning to the pores formed, there is evidence that oligomeric species are required. The high Hill coefficients are consistent with this interpretation, but would also be consistent with a rate-limiting direct transfer of oligomers (not monomers) from an aqueous aggregate to an active state in the bilayer. However, this oligomer transfer is inconsistent with the voltage clamp experiments in which the channels form from transporters held within the bilayer. A pathway *via* monomer insertion to the bilayer remains as both the simplest alternative and the one consistent with all data available. The fluorescence results are consistent with, but do not compel, a linkage between the observed excimer emission and the transport activity. Certainly, excimer emission is observed under conditions where transport can or does occur. And transport is only observed under conditions where excimer can also be observed. However, a direct correlation of excimer emission intensity with transport activity in vesicles is not possible in this system as the emission can also arise from the competing aqueous aggregate.

The voltage clamp data indicate that a wide range of transmembrane conducting species can be formed and that these species depend upon the electrolyte; more "regular" channels are observed with CsCl as electrolyte than with KCl. This suggests that transported ions are also essential in maintaining pore structure. This finding precludes some types of experiments that better defined ion channels will support. For example, the ionic selectivity of ion channels is typically determined from the "reversal potential";[1] this is not possible in this system as the nature of the species being probed is a function of the bathing electrolyte composition.

The location of the ***Dip*** unit plays a key role in channel formation. The most regular and stable conducting states are formed with the ***Dip*** unit located in the middle of the oligoester strand HO_2C-***X-Dip-Y-G(12)***–OH, followed by the carboxyl-terminal location. A location of the ***Dip*** adjacent to the hydroxyl terminus does not preclude the formation of conducting states, but these are uniformly short-duration "spikes" of highly variable conductance. The quenching data support a buried location for the membrane-bound ***Dip*** rather than a surface accessible site. The ***Dip*** could be accessible to water as part of a pore structure and would still not show quenching since the ion currents supported by these pores are high and the conjunction of an excitation at the time of a quencher passing nearby has a low probability.

The properties of a bilayer environment as a solvent constrain a discussion of the structures of the active species and their precursors. Although crystal structures of lipids show neatly tilted hydrocarbon chains arranged in bilayers,[47] molecular dynamics simulations and spectroscopic probes suggest a much more chaotic environment.[48] Nonetheless, individual lipid molecules retain a tilt with respect to the membrane normal on a time-average, and solutes with a long molecular axis dissolve in an orientation with the long axis aligned with the average orientation of the lipids.[49] Within the bilayer there is considerable motion, but headgroup, midpolar, and hydrocarbon regions are maintained in a time average.[2,3] The compounds discussed here can certainly fold on themselves, but in a membrane environment would be expected to align with the lipids as illustrated in the very idealized sketch in Fig. 6. The longest compound (HO_2C-***Dec-Dip-Hex-G(12)***–OH) is

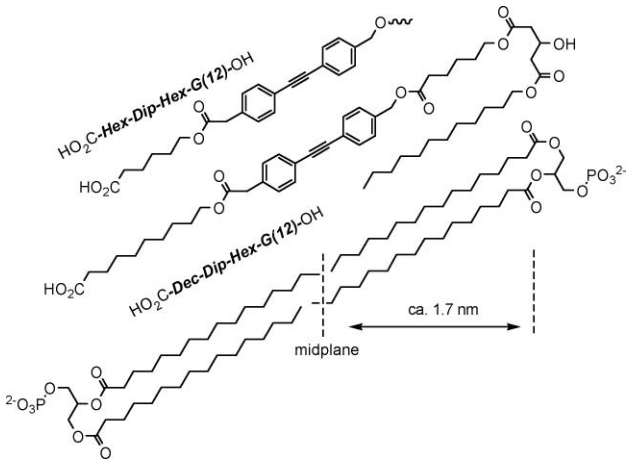

Fig. 6 Schematic of a transmembrane orientation of HO_2C-***X-Dip-Y-G(12)***–OH in comparison to an idealized lipid bilayer.

approximately the correct length to span the bilayer hydrocarbon region, The shorter HO_2C-***Hex-Dip-Hex-G(12)***–OH (illustrated in part in Fig. 6) would require some deformation and membrane thinning to span the bilayer, as is proposed for the well-studied gramicidin dimer channel.[50,51] In this type of transmembrane orientation, these positional isomers place the diphenylacetylene crossing the bilayer midplane. The other positional isomers in a similar orientation place the ***Dip*** within a single bilayer leaflet, leaving the more flexible methylene chains to cross the bilayer midplane. These transmembrane orientations are akin to lipid interdigitation in which a longer lipid molecule intrudes into the opposite leaflet.[52] In lipid systems, interdigitation leads to microphase separation and consequent rigidifying effects on lipid dynamics.[48]

The observed channels could be produced from this transmembrane orientation of monomer through a similar phase-separation mechanism. The separated domain would contain monomer in both possible orientations together with water, ions, and potentially a few lipid molecules. The differences between channels as a function of overall length, ***Dip*** position and electrolyte would then relate to the energetics and dynamics of these domains. The CsCl/HO_2C-***Dec-Dip-Hex-G(12)***–OH system produced small, well-defined but short-lived channels (Fig. 3(C)). This compound is the longest, so would require the least reorganization of the headgroups in order to attain a conducting state and could form and dissociate readily from a small phase-separated domain of a few molecules. The shorter homolog HO_2C-***Hex-Dip-Hex-G(12)***–OH produces longer-lived, and apparently larger channels (Fig. 3(A)/(B)) with lower probability reflecting a more challenging reorganization of the system before ionic conduction can occur. The more irregular behaviours observed with KCl electrolyte reflect the higher hydration energy of the cation in addition to any membrane reorganizations required. The result is a less defined domain that would allow highly variable transient pores to open/close quickly.

This picture of the channels formed in this type of system is more fluid than the proposals associated with larger and more conformationally constrained examples. Although many details remain obscure, the working hypothesis outlined in Fig. 1 appears to be well-supported by a range of direct and indirect probes. It is clear that the competing aqueous aggregate limits the activity of the compounds. Ongoing efforts to produce highly active pore-formers with this type of flexible lipophilic compound are directed to avoiding this species.

Experimental

General synthesis procedures

Most chemicals and solvents were used as received from known suppliers, except THF and DMF which were dried and distilled before use. NMR spectra were collected on a 300 MHz Bruker or 500 MHz Varian instrument. UV spectra were run on a Cary 5 UV-VIS spectrometer in a 10 × 10 mm quartz cell. ESI Mass spectra were recorded on a Waters MicroMass Q-TOF instrument running in negative ion mode. HPLC was performed using an HP Series 1100 instrument, with either a Macherey-Nagel "Nucleosil" RP C_{18} analytical (4 mm × 250 mm) or a Grace Davison "Alltima" RP C_{18} semi-prep (10 mm × 150 mm) column. Solvents used (ACN, CH_3OH; HPLC-grade, H_2O; Milipore) were filtered through a Milipore sub-micrometre filter before use. HPLC elution was monitored at various UV wavelengths (typically 254, 280 and 220 nm) and fluorometrically (λ_{ex} = 310, λ_{em} = 330 nm). Fluorescence spectra were run on a PTI QM-2 instrument at T = 20 °C, slit width = 3 nm in 10 × 10 mm quartz cells equipped with a micro stir rod.

Sonogashira coupling (***i***): To a round bottomed flask equipped with a septum, 1.2–1.5 equivalents (in relation to the alkyne starting material) of the iodo-containing reactant and 6–10% CuI were dissolved in dry DMF, which was then deoxygenated under vacuum. The alkyne reactant was then added to the flask, which was kept in the dark. $Pd(PPh_3)_4$ (3–5%) was then added, followed by 2–5 equivalents of NEt_3. The reaction was then stirred under N_2 at temperatures ranging from rt to 50 °C, for 10–24 h, depending on the reagents used. Reactions were monitored by TLC (silica gel, EtOAc/hexanes as eluent, visualized by UV, *p*-anisaldehyde and/or vanillin stain). Once complete, reactions were cooled if necessary, diluted with EtOAc and washed with saturated EDTA (2–3 times), H_2O (once), saturated NaCl (once), dried over sodium sulfate, and concentrated under vacuum. Unless noted otherwise, the crude products were purified by column chromatography on silica gel, typically using EtOAc/hexanes as eluent.

Ester coupling (***ii***): To a solution of 1.3–2 equivalents of either the alcohol or acid building block in relation to 1 equivalent of the other (excess reagent choice determined by ease of synthesis or availability) in THF or DMF (depending on substrate) were added 1.3–2 eq. of DIC, HOBt and 2.6–4 eq. of DIPEA. The reaction was sealed under an atmosphere of N_2, and stirred for 16–24 h at temperatures varying between rt and 50 °C. Reaction completion was monitored by TLC. Once complete, the reaction was cooled (if necessary), filtered to remove DIU, and diluted with DCM or EtOAc. The organic phase was extracted with H_2O (twice), saturated $NaHCO_3$ (twice), rinsed with sat NaCl (once), dried with anhydrous sodium sulfate, and concentrated under vacuum. Unless noted otherwise, the crude product was purified by column chromatography on silica gel, typically using EtOAc/hexanes as eluent.

THP removal (***iii***): pTsOH (5–25%) was added to a solution of compound in ~10–30% CH_3OH: DCM, which was stirred at rt

for 1–3 h, as monitored by TLC. Once complete, the reaction was diluted with DCM, washed with H_2O (once), saturated $NaHCO_3$ (twice), and saturated NaCl (once), then dried over sodium sulfate and concentrated under vacuum. If necessary, further purification was carried out as noted.

***Fluoride deprotection* (*iv*)**: ~5–10 equivalents of 1.0 M TBAF in THF were added to a solution of compound in THF, which was then stirred at rt for 1–3 h, as monitored by TLC. Once complete, the reaction was quenched by the addition of H_2O, diluted into EtOAc, washed with 10% aqueous HCl, (once), then H_2O (until neutral) and saturated NaCl (once), then dried over sodium sulfate and concentrated under vacuum. Further purification was carried out as noted.

***Prenyl deprotection* (*v*)** (adapted[53]): 0.025–0.1 equivalents TM-SOTf were added to the compound dissolved in DCM, which was stirred at rt. Once complete (as monitored by TLC, generally < 1 h), the reaction mixture was diluted further into DCM, washed with H_2O, saturated $NaHCO_3$ and saturated NaCl, then dried over sodium sulfate and concentrated under vacuum. Further purification was carried out as noted.

Spectroscopic and characterization data for all new compounds is given in the ESI.†

Transport studies

All samples used in transport experiments were HPLC-purified. The HPTS transport assay was done as previously reported;[20] minor changes to the published procedure include the use of a different buffer (100 mM NaCl, 10 mM $Na_3PO_4{\cdot}12H_2O$, pH ~6.4) and the injection of compound through a specially-designed injection port, which allows constant monitoring without the need for opening the instrument. Vesicles were made as reported, and sized on a Brookhaven Instruments ZetaPALS instrument. Average vesicle size was found to be ~180–200 μm. The experimental and data analysis systems for the voltage clamp experiments has been previously described.[40,41] All data were hardware filtered (8-pole Bessel filter, 1 kHz) and in a survey mode were filtered during acquisition at 1 kHz. The rapid spike and the flicker behaviors are near the 1 kHz limit and data for more detailed examination did not use the digital acquisition filter.

Fluorescence studies

All oligomers studied were purified by HPLC prior to use. Stock concentrations of approximately 1–6 mM in THF were stored under N_2 in the freezer when not in use, and periodically re-checked by HPLC. Volumes of compound in THF used in each experiment did not exceed 25 μL added into typically 2 mL of aqueous solution. The volume of solutions was kept approximately at 2 mL for all experiments. For studies in organic solvents, the solvents used were of spectral or higher quality, and were purged with N_2. For all aqueous studies except those involving $CuSO_4$, the aqueous buffer consisted of 10 mM $Na_3PO_4{\cdot}12H_2O$, 100 mM NaCl, pH = 6.4. For quenching studies with $CuSO_4$ in aqueous solution, either 100 mM unbuffered NaCl or 10 mM Bis-Tris, 100 mM NaCl, pH = 6.4 were used (as noted). Vesicles were prepared and sized as above, however, rather than always containing the HPTS dye, in certain cases, the vesicles were made with the same buffer both internal and external to the vesicle. Alternatively, for certain experiments, the compound was pre-incorporated into the vesicle bilayer by adding a solution of the compound of interest to the lipid mix before continuing the preparation as usual. Regardless of the identity of the vesicles, the volume of vesicle stock solution added to the cell was kept constant at 100 μL for each experiment.

Acknowledgements

The ongoing support of the Natural Science and Engineering Research Council of Canada is gratefully acknowledged.

Notes and references

1 S. Matile and N. Sakai, in *Analytical Methods in Supramolecular Chemistry*, ed. C. A. Schalley, Wiley-VCH, Weinheim, 2007, pp. 381–418.
2 G. W. Gokel and I. A. Carasel, *Chem. Soc. Rev.*, 2007, **36**, 378–389.
3 T. M. Fyles, *Chem. Soc. Rev.*, 2007, **36**, 335–347.
4 L. You, R. Ferdani, R. Li, J. P. Kramer, R. E. K. Winter and G. W. Gokel, *Chem.–Eur. J.*, 2008, **14**, 382–396.
5 C. P. Wilson and S. J. Webb, *Chem. Commun.*, 2008, 4007–4009.
6 L. Ma, M. Melegari, M. Colombini and J. T. Davis, *J. Am. Chem. Soc.*, 2008, **130**, 2938–2939.
7 M. Woodbury, M. M. Mongare, C. D. Hall, Z. Wang, B. Draghici, A. R. Katritzky, M. Tsikolia, A. C. Hall, C. Suarez, Z. O. Nylander, S. M. Wardlaw, M. E. Gibson, K. L. Valentine, L. N. Onyewadume and D. A. Ahove, *Org. Biomol. Chem.*, 2009, **7**, 3862–3870.
8 O. Lawal, K. S. J. Iqbal, A. Mohamadi, P. Razavi, H. T. Dodd, M. C. Allen, S. Siddiqui, F. Fucassi and P. J. Cragg, *Supramol. Chem.*, 2009, **21**, 55.
9 O. V. Kulikov, R. Li and G. W. Gokel, *Angew. Chem., Int. Ed.*, 2009, **48**, 375–377.
10 N. Illy, L. Bacri, J. Wojno, D. Destouches, B. Brissault, J. Courty, L. Auvray, J. Penelle and V. Barbier, *Macromol. Symp.*, 2010, **287**, 60–68.
11 A. Hennig, L. Fischer, G. Guichard and S. Matile, *J. Am. Chem. Soc.*, 2009, **131**, 16889–16895.
12 B. Gong, A. J. Helsel, A. L. Brown, K. Yamato, W. Feng, L. Yuan, A. J. Clements, S. V. Harding and Z. Shao, *J. Am. Chem. Soc.*, 2008, **130**, 15784–15785.
13 L. Ma, W. A. Harrell and J. T. Davis, *Org. Lett.*, 2009, **11**, 1599–1602.
14 S. Hagihara, L. Gremaud, G. Bollot, J. Mareda and S. Matile, *J. Am. Chem. Soc.*, 2008, **130**, 4347–4351.
15 X. Li, B. Shen, X.-Q. Yao and D. Yang, *J. Am. Chem. Soc.*, 2009, **131**, 13676–13680.
16 W. Wang, R. Li and G. W. Gokel, *Chem.–Eur. J.*, 2009, **15**, 10543–10553.
17 W. Wang, R. Li and G. W. Gokel, *Chem. Commun.*, 2009, 911–913.
18 X. Li, B. Shen, X.-Q. Yao and D. Yang, *J. Am. Chem. Soc.*, 2007, **129**, 7264–7265.
19 K. S. J. Iqbal, M. C. Allen, F. Fucassi and P. J. Cragg, *Chem. Commun.*, 2007, 3951–3953.
20 T. M. Fyles and H. Luong, *Org. Biomol. Chem.*, 2009, **7**, 733–738.
21 T. M. Fyles and H. Luong, *Org. Biomol. Chem.*, 2009, **7**, 725–732.
22 T. M. Fyles, C. Hu and H. Luong, *J. Org. Chem.*, 2006, **71**, 8545–8551.
23 T. M. Fyles, D. Loock, W. F. van Straaten-Nijenhuis and X. Zhou, *J. Org. Chem.*, 1996, **61**, 8866–8874.
24 T. K. Rostovtseva, C. L. Bashford, A. A. Lev and C. A. Pasternak, *J. Membr. Biol.*, 1994, **141**, 83–90.
25 T. Renkes, H. J. Schafer, P. M. Siemens and E. Neumann, *Angew. Chem., Int. Ed.*, 2000, **39**, 2512–2516.
26 T. M. Fyles, D. Loock and X. Zhou, *J. Am. Chem. Soc.*, 1998, **120**, 2997–3003.
27 P. Reiss, L. Al-Momani and U. Koert, *ChemBioChem*, 2008, **9**, 377–379.
28 G. A. Woolley, V. Zunic, J. Karanicolas, A. S. I. Jaikaran and A. V. Starostin, *Biophys. J.*, 1997, **73**, 2465–2475.
29 J. M. Kuiper, R. T. Buwalda, R. Hulst and J. B. F. N. Engberts, *Langmuir*, 2001, **17**, 5216–5224.
30 E. Abel, G. E. M. Maguire, O. Murillo, I. Suzuki, S. L. De Wall and G. W. Gokel, *J. Am. Chem. Soc.*, 1999, **121**, 9043–9052.
31 C. Ferrante, U. Kensy and B. Dick, *J. Phys. Chem.*, 1993, **97**, 13457–13463.
32 Y. Hirata, *Bull. Chem. Soc. Jpn.*, 1999, **72**, 1647–1664.

33 R. L. Letsinger, T. Wu, J.-S. Yang and F. D. Lewis, *Photochem. Photobiol. Sci.*, 2008, **7**, 854–859.
34 R. Chinchilla and C. Nájera, *Chem. Rev.*, 2007, **107**, 874–922.
35 P. J. Kocieński, *Protecting groups*, 3rd edn, Georg Theime Verlag, Stuttgart, 2005.
36 C. L. Kuyper, J. S. Kuo, S. A. Mutch and D. T. Chiu, *J. Am. Chem. Soc.*, 2006, **128**, 3233–3240.
37 M. E. Weber, P. H. Schlesinger and G. W. Gokel, *J. Am. Chem. Soc.*, 2005, **127**, 636–642.
38 *Single-channel Recording*, ed. B. Sakmann and E. Neher, New York, London, 1983.
39 T. M. Fyles and C. C. Tong, *New J. Chem.*, 2007, **31**, 655–661.
40 M. B. Buchmann, T. M. Fyles and T. Sutherland, *Bioorg. Med. Chem.*, 2004, **12**, 1315–1324.
41 P. K. Eggers, T. M. Fyles, K. D. D. Mitchell and T. Sutherland, *J. Org. Chem.*, 2003, **68**, 1050–1058.
42 B. Hille, *Ionic Channels of Excitable Membranes*, 3rd edn, Sinauer Associates, Incorporated, Sunderland, 2001.
43 K. Kalyanasundaraman and J. A. Thomas, *J. Am. Chem. Soc.*, 1977, **99**, 2039–2044.
44 H. Jiang, X. Zhao and K. S. Schanze, *Langmuir*, 2007, **23**, 9481–9486.
45 Y. Kobuke and K. Morita, *Inorg. Chim. Acta*, 1998, **283**, 167–174.
46 Y. Kobuke, K. Ueda and M. Sokabe, *J. Am. Chem. Soc.*, 1992, **114**, 7618–7622.
47 H. Hauser and G. Poupart, in *The Structure of Biological Membranes*, ed. P. L. Yeagle, CRC Press, Boca Raton, 2 edn, 2005, pp. 1–51.
48 K. Gawrisch, in *The Structure of Biological Membranes*, ed. P. L. Yeagle, CRC Press, Boca Raton, 2 edn, 2005, pp. 147–171.
49 J. M. Pope, L. W. Walker and D. Dubro, *Chem. Phys. Lipids*, 1984, **35**, 259–277.
50 G. A. Woolley and B. A. Wallace, *Journal of Membrane Biology*, 1992, **129**, 109–136.
51 O. S. Andersen, R. E. Koeppe and B. Roux, *IEEE Trans. NanoBiosci.*, 2005, **4**, 10–20.
52 J. L. Slater and C.-H. Huang, in *The Structure of Biological Membranes*, ed. P. L. Yeagle, CRC Press, Boca Raton, 2nd edn, 2005, pp. 122–145.
53 M. Nishizawa, H. Yamamoto, K. Seo, H. Imagawa and T. Sugihara, *Org. Lett.*, 2002, **4**, 1947–1949.